TRANSIENT DISTORTION AND nTH ORDER FILTERING IN DEEP LEVEL TRANSIENT SPECTROSCOPY (D^{n}LTS)†

C. R. CROWELL and S. ALIPANAHI

Departments of Electrical Engineering and Materials Science, University of Southern California, Los Angeles, CA 90007, U.S.A.

Abstract—Problems associated with intrinsic sensitivity and time constant selectivity of capacitive DLTS systems are discussed as well as intrinsic limitations in predominantly deep level doped semiconductors.

A previously published figure of merit for the optimized exponential correlator for capacitive DLTS studies is shown to be too high because of improper consideration of effects of level restoration: when correctly compared, a filter with a 12% lower figure of merit can be constructed based purely on gating and a weighted phase inversion before the integrator and a phase sensitive detector has a 20% lower figure of merit. The exponential DLTS correlator is also inadequate for analysis of continuous spectra because of its slow drop off in response ($\propto T_S$ for T_S shorter than the peak response time constant and $\propto T_S^{-1}$ for longer times). Blanking is necessary to achieve more selectivity relative to short time constants. When performed on-line, D^{2}LTS gives a response $\propto T_S^{-2}$ for longer times. Still more selective filters of order n, or D^{n}LTS, are considered based on weighted averages over time intervals in geometric progression that are suitable for DLTS and a system with ± 1 weighting and suitably chosen time intervals for use with DDLTS. For these filters there is no penalty in figure of merit associated with choice of DDLTS which also appears to be easier to achieve than DLTS. On-line filters with long time constant responses $\propto T_S^{-3}$ or higher order are shown to exact a large penalty in figure of merit. Equivalent filters can, however, be synthesized with much better figure of merit by a software compensation of multichannel data. The channels are then selected so that the responses of successive channels peak a factor of 2 away in T_S and the number of pulses used is decreased by a factor of two. Relative to a multipoint averager, the software compensated analyzer requires a factor of 100 less in measurement time for comparable accuracy when a spectrum must cover a range of 1000:1 in relaxation times. There are also comparable improvements in the holding time specifications and the number of A/D conversions if the system is to be coupled to a computer.

When the deep level concentration is comparable to the shallow doping concentration, the peak responses of both DLTS and DDLTS are broadened, the sensitivity increases, the response peaks are shifted to larger relaxation times, and the system becomes essentially nonlinear in response to the individual deep level constituents. This distortion can, in principle, be corrected by going to a constant capacitance mode of operation both during the initial driving pulse and during the recovery transient.

1. INTRODUCTION

The problem of capacitive analysis of deep level transients in semiconductor junctions is an interesting one both from a solid state point of view and as a problem in systems analysis. The expected signal is an exponential which can be repeated and easily measured by signal averaging techniques. Two relatively unique features, the lack of rapidly varying features in the long time portion of the transient and the experimenter's ability to cancel repetitively the effect of a portion of the initial response, leads to a simple system for optimization of data acquisition.

A variety of junction capacitance techniques has been used to study the electrical behavior of semiconductors in an effort to characterize their deep level impurities[1, 2]. Transient capacitance measurements can be used to acquire direct information concerning the emission time constants of the deep levels and their energy levels. Such measurements involve pulsing p–n junctions or Schottky diodes and examining the resulting transients. A direct point by point analysis of the transient is very time consuming and results in time-dependent errors in the measurement. For a more rapid technique, the introduction by Lang[3] of DLTS (Deep Level Transient Spectroscopy) using correlation techniques was a major contribution. In DLTS the transient is repeated many times and the capacitance $c(t)$ is measured with a box-car integrator at times t_1 and t_2 after the pulses. The difference signal, $[c(t_1) - c(t_2)]$, peaks when the impurity response time is of the order of $(t_2 - t_1)$. Such a filter provides a means of studying the spectrum of the emission time constants of deep centers in a given junction. From such measurements combined with appropriate control of the initial excitation a wealth of information can be acquired, namely, thermal capture cross-sections, thermal emission rates, energy levels, and doping concentration profiles. In an effort to facilitate spatial profiling of the deep levels. Lefevre and Schulz (LS)[4] introduced a differential DLTS (or DDLTS), a double "correlation" analysis in which signals from two different pulse amplitudes are analyzed on-line in an analogue system. In both techniques the transients to be

analyzed are the exponential recovery of the perturbed system to the initial deep level charge states. The excitation can be repeated and signal averaging techniques[5] used to look at portions of the recovery time spectrum. Kimerling[6] Fourier analyzed the resulting periodic transients by using phase-sensitive detection methods with the aid of a lock-in amplifier.

Miller, Robinson and Ramirez (MRR)[7] looked at DLTS in fairly detailed terms and established a figure of merit guideline for the performance of different measurement systems. The major feature of their figure of merit was the signal to noise ratio (S/N) that could be obtained for a given measurement time. Selectivity with respect to emission time constant was included, but the systems they considered varied so little in selectivity that this consideration was relatively minor. MRR compared the box-car, phase-sensitive detection, linear ramp, and exponential correlator systems and concluded that the exponential correlator is best and is a factor ~2 better than phase-sensitive detection. The linear ramp filter lies somewhere between the two. In this paper we examine their guidelines in more depth. MRR introduced an extra feature to reject d.c. signals in their exponential correlator. They "restored" their signal by subtracting its value at the end of one pulse from the signal in a succeeding pulse. For a more realistic calculation of S/N we consider here the noise due to the restoration process to reject a d.c. signal. When performed rapidly the restoration process is noisy and degrades the S/N[8,9]. This was not considered by MRR in arriving at their figure of merit. Since all the schemes suggested by MRR have a low $Q(\sim 1/2)$†, in this paper we discuss methods of improving the selectivity of the overall system. This is absolutely essential when, instead of a single time constant, a distribution of time constants is investigated. Our technique makes the deconvolution of the time constants relatively simple and easy to interpret. Our approach is a hybrid of the multipoint averaging technique and the single channel box-car averager. We also suggest some guidelines that permit one to analyze distortion effects in the deep level transients when the deep level concentration is an appreciable fraction of the total doping.

2. THEORETICAL BACKGROUND

The basic signal to be detected in DLTS is an exponential signal of time constant T_S from the incremental capacitive response to a controlled pulse excitation. A signal of exponential shape $f(t)$ buried in noise $n(t)$ and other exponentials can be retrieved by a correlator. The amplitude A and time constant T_S can be obtained by multiplying the in-coming signal $Af(t)$ with a weighting function $w(t)$ and integrating the result. If the correlation is measured over a time T_M, the resultant output, E, is

$$E = \int_0^{T_m} (Af(t) + n(t))w(t)\,dt. \qquad (1)$$

It is well established that when the noise is white, then the signal to noise ratio at the output of the correlator is a maximum when $w(t)$ has the same shape as $f(t)$. This situation is modified when a finite time, T_M, is available to analyze a single pulse. Then for an exponential weighting function of time constant T_R, the correlator will have a peak response for $T_S = T_R$ in general only when the ratio T_R/T_M has a specific value. Also, in practice, in order to achieve selectivity in the output of the correlator there is a primary need for rejection of a constant background signal, i.e. for restoration. MRR tried to achieve this restoration by making a pseudo-instantaneous measurement of the incoming signal at time T_M and subtracting it from the signal. In other words, their response is actually E' where

$$E' = \int_0^{T_M} (f(t) + n(t) - f(T_M) - n(T_M)) \cdot w(t)\,dt. \qquad (2)$$

In effect the signal to be detected has now become $(f(t) - f(T_M))$. MRR did not use a weighting function of the form $(f(t) - f(T_M))$, but nevertheless succeeded in peaking their response at $T_S = T_R$ by appropriate choice of the ratio T_R/T_M. MRR neglect any contribution from $n(T_M)$. Strictly speaking an instantaneous rms expectation value of noise cannot be defined: the shorter the time available to determine $(f(T_M) + n(T_M))$ the more the S/N suffers. Miller et al.[10] later discussed the use of a finite time to determine $f(T_M)$ but did not consider its effect on a figure of merit either with respect to added noise or time to acquire the information. "Slow" restoration, where $f(T_M)$ or its equivalent is established by a separate experiment is assuredly less noisy than the "fast" restoration discussed above but also carries an added time for measurement and worry about long term drifts. We discuss the figure of merit for slow restoration elsewhere[11] and show that a slow restoration system in principle cannot have a better figure of merit than a correspondingly optimized correlator in which restoration does not require signal sensing. The problem of restoration can best be treated as follows. If $w(T)$ is chosen so that

$$\int_0^{T_M} w(t)\,dt = 0,$$

then a constant signal will be rejected. The d.c. rejection can thus be accomplished at the same time as the signal is acquired. The signal part, S, of the correlator output for a channel integration time T_C is

$$S = \int_0^{T_C} f(t) \cdot w(t)\,dt \qquad (4)$$

and the resulting rms noise, n_{rms}, is

$$\frac{n_{rms}}{K} = N = \left[\int_0^{T_C} w^2(t)\,dt \right]^{1/2} \qquad (5)$$

where K is a constant of proportionality and N is thus a normalized noise. The origin of eqn (5) is reviewed in

---

† We propose here a definition of Q analogous to that of a resonant system; namely, the ratio of the time constant for peak response to the difference in response times of amplitude 3dB from the peak.

Appendix A. If $f(t)$ and $w(t)$ are repetitive functions with a period that is a submultiple of T_C, the signal S is proportional to T_C while the noise N is proportional to $\sqrt{T_C}$. From the above it follows that a figure of merit for the system is

$$F \equiv \frac{S_{max}}{N\sqrt{T_C}} \tag{6}$$

where S_{max} is the peak sensitivity.

3. SINGLE CHANNEL SPECTRUM ANALYZERS

3.1 DLTS

The correlation of an unknown signal $f(t)$ with a weighting function $w(t)$ can enhance the S/N considerably[12]. In theory when $w(t) \equiv f(t)$, i.e. when the weighting function identically matches the form of the signal, then the S/N is a maximum. Unlike the MRR system that uses a measurement of $f(T_M)$, when the weighting function is a d.c. restored exponential of time constant T_R, the correlation with a signal of time constant T_S yields a maximum S/N when $T_R = T_S$. We have determined by inspection that for a given measurement time per pulse, T_M, the optimum choice of T_R for a spectrum analyzer is $0.31\ T_M$. Figure 1 lists numerous weighting functions $w(t)$ with their corresponding figures of merit and T_M/T_S ratios at maximum sensitivity. For a linear DLTS filter we also include two other asymmetrical weighting functions, namely the linear ramp and the rectangular. Their spectral responses are shown in Fig. 2. F for the linear ramp almost matches that for the optimum exponential correlator. The rectangular weighting which essentially acquires the signal in $T_M/4$ and spends the remaining $(3T_M/4)$ rejecting a constant signal is very close to the optimum rectangular weighting which

occurs for $\lambda = 0.28$ (see Fig. 1). Unlike the MRR modelling result in which noise associated with restoration is ignored, this filter does surprisingly well with only a 12% penalty in S/N relative to the exponential correlator. This result is fortunate in view of the fact that this filter can be realized without a multiplier: the only prerequisite is timing control circuitry that employs fast and reliable gating.

The algebraic expressions for signal and noise for the different weighting functions are included in Appendix B. Figure 2 is a plot of the normalized signal to noise ratio as a function of T_M/T_S. It is clear from such a plot that the responses with the asymmetrical weighting functions exhibit a filter that goes as T_S^{-1} in the long time constant portion of the spectrum and as T_S for short time constants. They all possess broad shoulders and Q's of the order 0.5.

3.2 DDLTS

The remaining weighting functions in Fig. 1 are automatically restored since all satisfy the condition

$$w(t) = -w(t + T_M/2). \tag{7}$$

This allows them to be used for DDLTS in which a second excitation pulse of different amplitude is introduced at time $T_M/2$. The fundamental individual measurement consists of a repeated sequence of events over a time T_M. In this category the exponential correlator attains the highest S/N followed by the square wave weighting. The output spectral responses are shown in Fig. 3. Both exhibit selectivities that are similar to those of the DLTS filters. We also consider two box-car weighting functions, one with $T_M/10$ blanking time and the other with $T_M/4$ blanking. From Fig. 1 the box-car with smaller blanking time has S/N almost 50% better, but has the effect of shifting the response fall off to shorter time constants. These filters exhibit a sharp exponential drop due to the blanking process which effectively filters out fast decaying transients. The sine wave does modestly in S/N with a 30% penalty as compared to the S/N for the exponential filter, but has the interesting characteristic of falling as T_S^2 in the short time constant spectrum.

The last three weighting functions in Fig. 1 have the additional property of being symmetrical with respect to $t = T_M/2$, i.e.

$$w(t) = w(T_M - t). \tag{8}$$

Their lineshapes go as T_S^{-2} in the long time constant limit and as T_S in the short time constant portions of the spectrum (see Fig. 3). These filters not only reject constant signals, but also reject any linear drift over the time T_M. This can be associated with temperature dependent transients that may exist during the measurement process. It is true from Fig. 1 that by the time we go down to a second order filter (T_S^{-2}) the S/N degrades more than a factor of 2, but considering that experimental drifts and heating effects occur, such second order or even higher order filters may be desirable for measure-
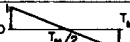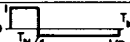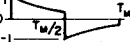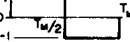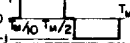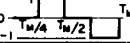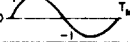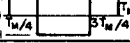
TYPE	FILTER	WEIGHTING FUNCTION	$\frac{T_M}{T_S} @ S_{max}$	F
D L T S	T_S^{-1}	EXPONENTIAL	3.2 $(T_S = T_R)$	.257
		LINEAR RAMP	2.7	.241
		RECTANGULAR	3.3 $(\lambda = .28)$	.225
D D L T S	T_S^{-1}	EXPONENTIAL	3.16 $(T_S = T_R)$	.218
		SQUARE WAVE	2.5	.208
		BOX CAR $T_M/10$ BLANKING	2.1	.160
		BOX CAR $T_M/4$ BLANKING	1.7	.108
		SINE	2.35	.178
	T_S^{-2}	COSINE	6.4	.112
		TRIANGULAR	6.5	.114
		QUADRATURE SQUARE WAVE	6.3	.096

Fig. 1. A variety of weighting functions suitable for DLTS and DDLTS filters with their corresponding location of peak sensitivity and figure of merit F.

RESTORED   WEIGHTING   FUNCTIONS

F	EXPONENTIAL	F	LINEAR	F	CONSTANT
.257		.241		.225	

Fig. 2. Normalized S/N as a function of T_M/T_S for three asymmetrical weighting functions: Exponential, linear and rectangular.

SELF-RESTORED   WEIGHTING   FUNCTIONS

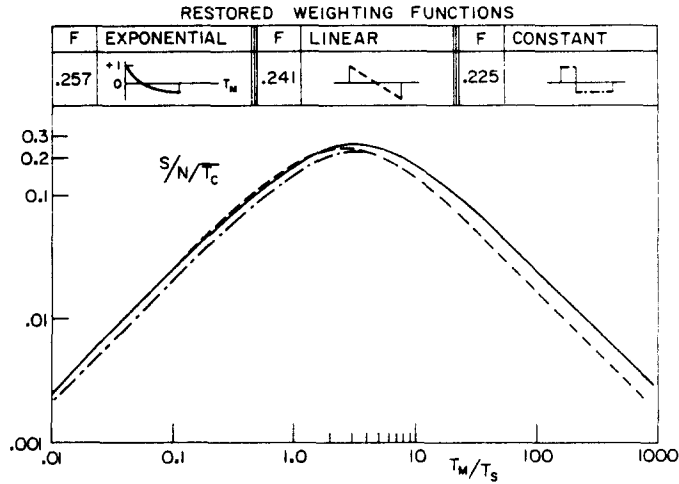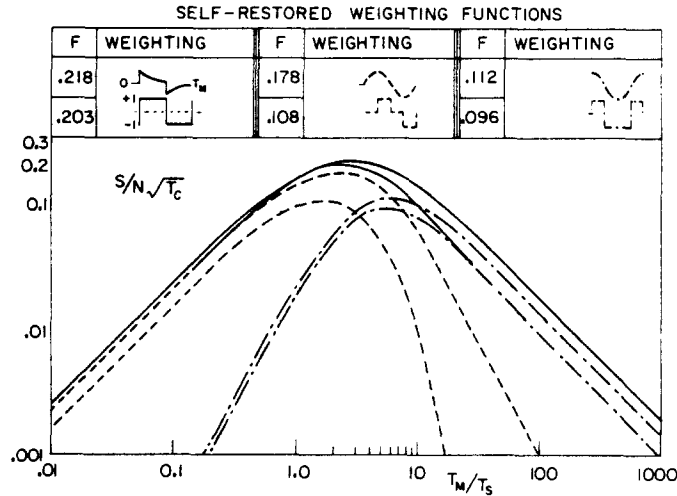| F	WEIGHTING	F	WEIGHTING	F	WEIGHTING
.218		.178		.112	
.203		.108		.096	

Fig. 3. Normalized S/N as a function of T_M/T_S for six automatically restored weighting functions: Exponential, square, sine, box-car, cosine and quadratic square wave. The spectral responses can be correlated to their weighting functions because F is the peak response.

Table 1. Values of λ for derived filters

Derived filter	Fundamental filter Unrestored (T_s^0)				Restored (T_s^{-1})			2nd order (T_s^{-2})	
	λ_2	λ_4	λ_8	λ_{16}	λ_2	λ_4	λ_8	λ_2	λ_4
T_s^{-1}	-1	0	0	0	0	0	0	—	—
T_s^{-2}	$-\dfrac{3}{2}$	$\dfrac{1}{2}$	0	0	$-\dfrac{1}{2}$	0	0	0	0
T_s^{-3}	$-\dfrac{7}{4}$	$\dfrac{7}{8}$	$\dfrac{1}{8}$	0	$-\dfrac{3}{4}$	$\dfrac{1}{8}$	0	$-\dfrac{1}{4}$	0
T_s^{-4}	$-\dfrac{15}{8}$	$\dfrac{35}{32}$	$\dfrac{15}{64}$	$\dfrac{1}{64}$	$-\dfrac{7}{8}$	$\dfrac{7}{34}$	$\dfrac{1}{64}$	$-\dfrac{3}{8}$	$\dfrac{1}{32}$

ment systems. By examining the different weighting functions it becomes clear that blanking is absolutely necessary for a sharp fall off in the short time constant portion of the spectrum. The long time constants can be filtered on-line by appropriately selecting the weighting function. For this purpose we consider two classes of weighting functions. In one class, after blanking the response for $T_M/10$, the remaining 0.9 T_M is divided into geometric intervals of 1, 2, 4... with the proper choice of weightings as shown in Fig. 4. These weighting functions are suitable for DLTS. In the other class, T_M is divided into tenths with switches in weighting at intervals of 1, 5,

ON-LINE FILTERS WITH BLANKING

Fig. 4. Higher order on-line filters with blanking suitable for DLTS and DDLTS with their weighting functions accompanied by the location of peak sensitivity and figure of merit F.

6, 10; 1, 3, 5, 6, 8, 10; and 1, 2, 4, 5, 6, 7, 9, 10 and only unity gains are used. This system is suitable for DDLTS. Our calculations show that the DDLTS weightings do slightly better in figure of merit as compared to the DLTS. Also from an engineering point of view, precision unity gain is easier to achieve than the fractional gains used in the alternative approach. The time intervals can be basically derived from a clock and counter. The results of the figure of merit indicate that by the time we go to a third order filter (T_S^{-3}), we pay a factor ~ 10 in S/N or a factor of 100 in measurement time as compared to the first order filter (T_S^{-1}).

4. NOMENCLATURE FOR SINGLE CHANNEL ANALYZERS

As is apparent from the preceding section, on-line filters result in figures of merit that are probably prohibitively low for most applications. In an effort to remedy this situation, we propose in Section 4 a multichannel approach where the S/N is kept reasonably high in each channel when the signal is acquired and the information is combined from adjacent channels with software compensation. We can then arrive at more selective lineshape by paying only a modest penalty in the overall S/N.

We would like first, however, to develop an appropriate nomenclature to describe such a filter. A descriptive term for a filtering system with a long time constant response proportional to T_S^{-n} is D^{n}LTS: it requires the equivalent of n two-channel filters and detects the exponential signal solely on the basis of terms of higher order than n in the exponential signal. Higher order systems have considerable merit when one considers that extraneous signals can easily simulate a portion of an exponential. A filter with $n = 1$ rejects d.c. signals, $n = 2$ linear drifts, $n = 3$ quadratic drifts, etc. The selectivity also increases with the order. In the past the

terms DDLTS and D^{2}LTS have been used to describe the LS system. In actual fact there are two potential reasons for this choice. The subtraction of signals from two pulse amplitudes makes the system a differential one regardless of whether or not a two-correlator system is used. We propose here that the term DDLTS be used generically for a differential pulse method and that the term D^{n}LTS be reserved to describe the temporal selectivity of the system, i.e. DDLTS is a differential deep level transient spectroscopy with an implied long time constant fall off αT_S^{-1}.

The LS[4] system within the above nomenclature would be DD^{2}LTS. This statement requires amplification. LS set up a system to provide an on-line spatial resolution of DLTS signals. The LS DDLTS analysis used a two pulse sample measurement sequence with a double box-car weighting in each pulse (see Fig. 1). The integrated signal from the smaller of two pulses was subtracted from the integrated signal from the subsequent larger pulse. In this sequence the larger pulse erases all memory of the response to the smaller pulse. If averaging is done on one such sequence then the filter response would be of first order (T_S^{-1}). With the pulse sequence reversed, there is, however, an added temporal selectivity; the smaller pulse overrides a portion of the original signal but part of the signal from the larger pulse remains and contributes to make the system a second order filter (T_S^{-2}). This is treated in detail in Section 5. The upper limit to the LS on-line filter thus has a figure of merit ~ 0.05 (assuming that in reality it was a T_S^{-2} filter).

5. ANALYSIS OF A COMPLETE SPECTRUM

The analysis we have just presented can be used to extract the information that a signal lies in a given portion of a relaxation time spectrum. If we wish to use such an analyzer to scan a spectrum there are a few general guidelines that we should observe. Because all of the systems have a relatively low quality factor we should not make measurements with channel separation less than approximately $\Delta T_S / T_S \sim 2$. Accordingly successive scans with $T_M = T_{M_1}, 2T_{M_1}, 4T_{M_1}, \ldots$ will yield all the basic information that is available. In order that the measurements have the same sensitivities and same nominal rms noise content it is necessary that T_C, the total time for signal acquisition, be invariant. Thus the number of pulse repetitions for these measurements must go as $r = r_1, r_1/2, r_1/4, \ldots$ The number of pulse repetitions needed for a signal with a large T_S is very small relative to that needed for a signal with a small T_S. This fact can be exploited to analyze a complete spectrum with a considerable saving in time over an approach that uses an on-line multipoint analyzer. In the rest of this section we show how one can take the above succession of single channel measurements and make a software correction of the measurements. We can thus obtain a T_S^{-2} or higher order filter with only a modest penalty in the figure of merit associated with the derived data. This system is a dramatic improvement over attempts to use an on-line higher order filter. One of the basic reasons for this is the use of equal dwell time

within the acquisition time, T_C, per channel to produce data of uniform sensitivity and noise across the complete spectrum. Let us now consider how we can use such multiple channel measurements to produce a set of software compensated data such that the derived data will be associated with a sharper spectral response than the initial measurement. Let the response in channel 1 be $s_1 = s(x)$ for a given $x = T_M/T_S$. Then the response in channel 2 for the same T_C is $s_2 = s(2x)$ and that in channel 3 is $s_3 = s(4x)$, and so on. The derived weighted response from such a multichannel system is

$$S_{MC} = s(x) + \lambda_2 s(2x) + \lambda_4 s(4x) + \lambda_8 s(8x) + \cdots$$
(9a)

where $\lambda_2, \lambda_4, \lambda_8, \ldots$ can be chosen to yield a desired spectral response. The corresponding expectation value of the rms normalized noise is

$$N_{MC} = N_1(1 + \lambda_2^2 + \lambda_4^2 + \cdots)^{1/2}$$
(9b)

where N_1 is the rms noise in the fundamental channel. The figure of merit, F_{MC}, that is analogous to the single channel figure of merit is

$$F_{MC} \equiv \frac{S_{MC(max)}}{N_{MC}} \sqrt{\left(\frac{1+m-n}{mT_c}\right)}$$
(9c)

where m is the number of channel measurements made and n is the number of channel measurements combined to yield a corrected datum. The total measurement time is mT_c and the total number of data points obtained is $(1 + m - n)$. The above is a conservative figure of merit because we assume that the last $(n - 1)$ channels used to measure the long time constant response will only be used to correct the data at shorter time constants. We have shown that appropriate blanking can control the short T_S fall-off of the response. We now show how choice of the λ's can control the long T_S fall-off. We can

expand $s(x)$ in a polynomial form as follows

$$s(x) = a_0 + a_1 x + a_2 x^2 + \cdots$$
(10)

If $a_0 \neq 0$, the fundamental single channel response does not reject a constant signal ($x = 0$ for a constant signal). To reject d.c., i.e. to make the contribution of a_0 zero in S_{MC}, we must have

$$1 + \lambda_2 + \lambda_4 + \cdots = 0.$$
(11)

To reject also linear drifts, i.e. the effects of a_1 in S_{MC}, we must further satisfy

$$1 + 2\lambda_2 + 4\lambda_4 + \cdots = 0.$$
(12)

To reject quadratic variations, i.e. a_2 terms, we need in addition the condition

$$1 + 2^2\lambda_2 + 4^2\lambda_4 + \cdots = 0.$$
(13)

Solutions for a variety filters follow from satisfying the above set of linear equations. Representative λ's are listed in Table 1.

Let us apply our multichannel approach to a simple basic gating function which blanks to $T_M/2$ and provides unity gain between $t = T_M/2$ and T_M. We plot the spectral response of the filters so obtained in Fig. 5 and list their corresponding figures of merit. Since the fundamental response cancels neither d.c. imbalances nor drifts, this might well be a difficult system to use in practice. Nevertheless the spectral responses show that higher order filtering can be achieved without incurring a substantial degradation in the figure of merit as compared to on-line single channel filters (see Fig. 5). When we employ a weighting suitable for DDLTS, there is no response to a constant signal. Thus $s(x)$ has no constant term ($a_0 = 0$). The required values of λ can be chosen to exploit this feature to improve the figure of merit. The

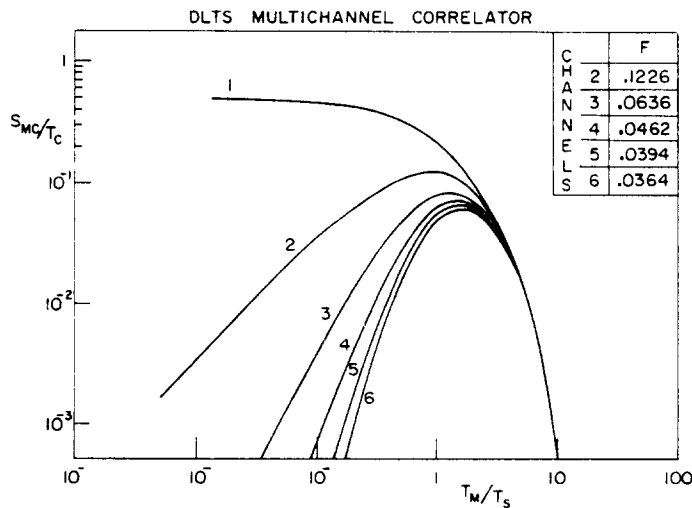| C H A N N E L S	F
2	.1226
3	.0636
4	.0462
5	.0394
6	.0364

Fig. 5. Normalized signal S_j/T_C of unrestored software compensated DLTS multichannel system for higher order filters (first to fifth order) as a function of T_M/T_S.

new λ's (λ') bear a simple relation to the old λ's (λ) via the relation $\lambda'_n = \lambda_n/n$.

Figure 6 shows a plot of the derived signal S as a function of T_M/T_S for box-car weighting functions with $T_M/10$ blanking time and with $T_M/4$ blanking. In this case when we produce a third order derived filter we only pay a factor $\simeq 2.2$ in figure of merit relative to on-line single channel filters where we had to pay a factor ~ 10 to produce an active third order filter (see Fig. 4). The results of our calculations for the case $m \gg (n - 1)$ (see eqn 9c) are listed in Table 2 and provide a basis for comparison of different spectrum analyzers. Relative to software compensated multichannel analyzers the figure of merit of on-line single channel analyzers degrades drastically as we go to higher order filters. In the multichannel systems the signal is basically acquired at the sensitivity of the fundamental filter and the figure of merit degradation is modest. This improvement is predicated on the use of a large enough number of channels that the use of data from two or three channels to obtain a single channel datum does not represent an appreciable time increment. If, however, we combined two or three channels to obtain only an equivalent single channel response (i.e. $n = m$ in eqn (9c), we would find that our multichannel weighted system is still superior to the on-line single channel analyzers. A comparison of the figures in columns 1 and 3 of Table 2 show that for

higher order filters the software-compensated system has much to recommend it.

A possibly surprising result is that the figure of merit for DLTS and DDLTS are very similar in spite of the fact that in DDLTS we achieve a spatial resolution as well as a temporal resolution during a single measurement sequence over a time T_M. This point is considered in detail in Section 6. The reason for the similarity is that in DLTS the time required for restoration is virtually equivalent to the corresponding time which in DDLTS is simultaneously devoted to (automatic) restoration and spatial resolution. The order of the large and small pulses in DDLTS is important if the pulse sequences are widely separated in time. This key point can also be appreciated by a detailed consideration of Section 6 and is relevant to the LS measurements.

Our multichannel (MC) approach offers a very considerable saving in time relative to a multipoint averaging (MPA) system which is normally considered to be faster than a succession of single channel measurements[13]. The MPA system samples the spectrum with a selection of gates T_{min} wide over a fundamental period of time T_{max} where we can define the corresponding number of the MC channels, m, by the relationship
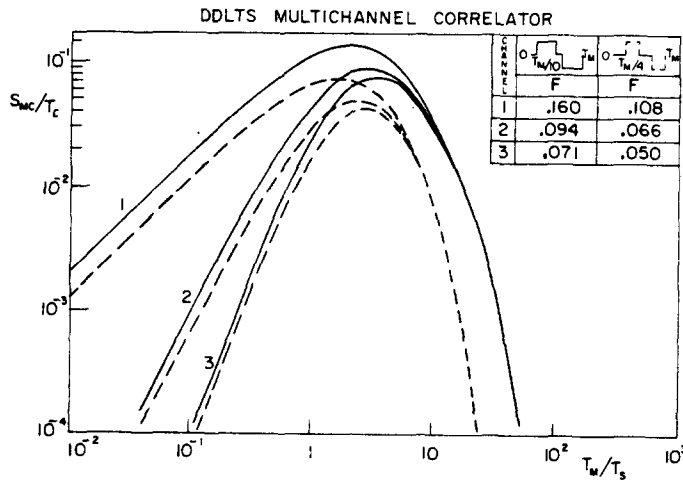
$$T_{max} = 2^{m-1} T_{min}. \tag{14}$$

Fig. 6. Normalized signal S_j/T_C of two box-car weighting functions ($T_M/4$ and $T_M/10$ blanking time) for software compensated DDLTS multichannel systems for higher order filters (first to third order) as a function of T_M/T_S.

Table 2. Figure of merit comparison of on-line single-channel with software compensated multichannel DDLTS system with $T_m/10$ blanking (see Figs. 4 and 6)

Type of filter	On-line single channel	Software compensated multichannel	Software compensated single channel
T_s^{-1}	0.160	0.160	0.160
T_s^{-2}	0.050	0.094	$\dfrac{0.094}{\sqrt{2}} = 0.066$
T_s^{-3}	0.015	0.071	$\dfrac{0.071}{\sqrt{3}} = 0.041$
T_s^{-4}	0.0037	0.062	$\dfrac{0.062}{2} = 0.031$

The MPA scheme requires a total acquisition time

$$T_{MPA} = \left(\frac{T_C}{T_{min}}\right) T_{max} \tag{15}$$

to have a potential S/N equal to that of the multichannel analyzer.

Our proposed multichannel (MC) system, employs sampling gates that are $T_{min}, 2T_{min}, 4T_{min}, \ldots, 2^{m-1}T_{min}$ wide. The MC system then requires a total acquisition time of

$$T_{MC} = mT_c \tag{16}$$

thereby reducing the acquisition time required for the analysis of a complete spectrum by a factor $2^{m-1}/m$ where m is the number of channels. For large m, it is clear that this factor is large (≈ 100 for $T_{max}/T_{min} = 1000$). This results in a dramatic savings in time for a given S/N ratio. Note that if the gates are made wider for larger time values we will need less time than specified above for the larger time constants in the MPA scheme, but the resolution will be lacking to determine the shorter time constant contributions. Another systems advantage is the number of A/D conversions required for the storage of data. For analogue signals the holding time is $(T_C/T_{min})T_{max}$ for the MPA system and T_C for the MC system. For a digital acquisition of the information we would require $m(T_C/T_{min})$ conversions for the MPA system (presuming the same gate spacing as in the MC system) as opposed to m conversions for the MC system. For studying very short response times the MC approach might well make it possible to use an on-line digital acquisition system where the net channel response is digitized as opposed to a system where digitizing each individual pulse would require too rapid a transfer of information.

6. DISTORTION OF THE DEEP LEVEL TRANSIENT

A signal analysis using DDLTS is presented here for a metal n-type semiconductor of shallow dopant of density N_s containing a deep impurity level of doping N_d and energy level E_{DD} as shown schematically in Fig. 7(a). The DDLTS analysis of the deep level was first presented by Lefevre and Schulz[4]. We wish to extend their analysis in more detail and show the effect of the deep level on the spectrum when N_d in an appreciable fraction of N_s. In DLTS the reverse biased diode at voltage V_B is pulsed towards zero bias with a positive-going pulse of height V_1. Let us look at the subsequent transient after the removal of the pulse (see Fig. 7b). The capacitance signal comes from the motion of the depletion layer a distance δw_{01} and occurs because at bias V_B a positive charge due to the change in depletion width is needed to balance the effect of the added negative charge on the deep level species. This changes the Fermi level crossover point of the deep impurity from x_{c0} at bias V_B to x_1 at bias $V_B - V_1$. During the recovery transient (see Fig. 7c), the crossover moves to $x_{c0} + \delta x_{c1}(t)$ where $\delta x_{c1}(t) \approx \delta w_{01}(t)$ if the shallow dopant is constant. Thus there is a build up of positive charge about the crossover point
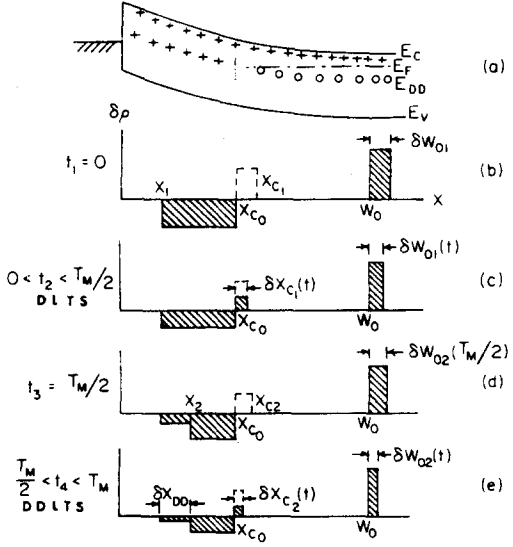

Fig. 7. (a) Schematic energy band bending for a metal-n type semiconductor Schottky diode containing a deep impurity level of energy E_{DD}. (b) The change in charge density, $\delta\rho$ (relative to steady state at voltage V_B), as a function of x immediately after the applied voltage changes from $V_B - V_1$ to V_B. The deep level crossing of the Fermi energy has just changed from x_1 to x_{c1}, from its steady state value at x_{c0}. (c) Incremental charge distribution at time t_2: $0 < t_2 < T_M/2$. (d) Distribution after applying and removing a bias increment V_2 at time $t_3 = T_M/2$. (e) Incremental charge distribution at time t_4: $t_4 = T_2 + T_M/2$.

which in turn does not remain fixed in time. In DDLTS, introducing a second positive-going pulse of height V_2, where $V_2 < V_1$, at time $t = T_M/2$ results in narrowing down the region of interest in the depletion layer and provides the possibility of spatial profiling. Figures 7(b)–(e) show the change in charge density developed in the depletion region as a function of x, the distance from the metal, for four subsequent times; $t_1 = 0$, $0 < t_2 < T_M/2$, $t_3 = T_M/2$, and $t_4 = t_2 + T_M/2$. Immediately at the end of the first pulse, V_1, there is no deep level charge for $x \geq x_1$. The equation for the band bending is

$$\frac{\epsilon}{q}(V_B - V_1 - V_{dB}) = \int_0^{x_1} (N_s + N_d)x \, dx + x_1 \int_{x_1}^{w_{1f}} N_s \, dx. \tag{17}$$

where x_1 is the Fermi level crossover point due to V_1, w_{1f} is the depletion width edge associated with this forward drive and V_{dB} is the band bending associated with bulk conduction band relative to the deep level crossover by the bulk Fermi energy. The charge left in the region affected by the first pulse but not by the second pulse also modulates the effect of the second pulse. At the end of the second pulse, V_2, the new band bending equation yields

$$\frac{\epsilon}{q}(V_B - V_2 - V_{dB}) = \int_0^{x_1} (N_s + N_d)x \, dx + \int_{x_1}^{x_2}$$
$$\times [N_s + N_d \cdot (1 - \exp{-(T_M/2T_S)})]x \, dx + x_2 \int_{x_2}^{w_{2f}} N_s \, dx \tag{18}$$

where w_{2f} is the depletion layer edge and x_2 the deep level crossover. Now

$$\frac{\epsilon V_{dB}}{q} = \int_{x_1}^{w_{1f}} N_s(x - x_1)\,dx = \int_{x_2}^{w_{2f}}$$

$$\times N_s(x - x_2)\,dx = \int_{x_{c0}}^{w_0} N_s(x - x_{c0})\,dx. \tag{19}$$

Thus for constant N_s

$$w_{1f} - x_1 = w_{2f} - x_2 = w_0 - x_{c0} \equiv \delta x_d. \tag{20a}$$

The deep level segment studied in DDLTS is of width δx_{DD}, where

$$\delta x_{DD} \equiv x_2 - x_1. \tag{20b}$$

After subtracting eqn (18) from eqn (17), we obtain

$$\frac{\epsilon}{q}(V_1 - V_2) = \int_{x_1}^{x_2} [N_s + N_d(1 - \exp - (T_M/2T_S))]$$

$$x\,dx + N_s\delta x_{DD}\delta x_d. \tag{21}$$

For a voltage increment $\delta V (\equiv V_1 - V_2)$ that is small enough for the doping concentrations to be constant over the incremental distances,

$$\delta_{x\,DD} =$$

$$\frac{\epsilon\delta V}{q\left[(N_s + N_d)\dfrac{(x_1 + x_2)}{2} + N_s\delta x_d\right][1 - \lambda_d \exp - (T_M/2T_S)]} \tag{22}$$

where

$$\lambda_d \equiv \frac{1}{1 + \dfrac{N_s}{N_d}\left[1 + \dfrac{2\delta x_d}{x_1 + x_2}\right]}. \tag{23}$$

Note that for a given δV, the width of the region examined is a function of T_M/T_S unless $\lambda_d \ll 1$. λ_d is a parameter that is dependent on N_d/N_s and the drive voltages $(V_B - V_1)$ and $(V_B - V_2)$.

At a time t after the first pulse

$$\frac{\epsilon}{q}(V_B - V_{dB}) = \int_0^{x_1} (N_s + N_d)x\,dx + \int_{x_1}^{x_{c1}}$$

$$\times [N_s + N_d(1 - \exp - (t/T_S))]x\,dx + N_s x_{c1}(t)\delta x_d, \tag{24}$$

where $x_{c1}(t)$ is the new crossover point of the deep level. $w_{01}(t)$, the corresponding depletion layer edge occurs at $x_{c1}(t) + \delta x_d$.

During recovery from the second pulse, the transient

response is described by

$$\frac{\epsilon}{q}(V_B - V_{dB}) = \int_0^{x_1} (N_s + N_d)x\,dx$$

$$+ \int_{x_1}^{x_2} [N_s + N_d(1 - \exp - (t/T_S))] \times x\,dx$$

$$+ \int_{x_2}^{x_{c2(t)}} [N_s + N_d(1 - \exp - (t - T_M/2)/T_S)]x\,dx$$

$$+ N_s x_{c2}(t)\delta x_d. \tag{25}$$

Subtracting the resulting transient responses and using as time references $t = 0$ and $t = T_M/2$ for the first and second signals respectively,

$$\int_{x_1}^{x_2} N_d \exp(-t/T_S)(1 - \exp - T_M/2T_S)x\,dx$$

$$= \int_{x_{c2(t)}}^{x_{c1(t)}} [N_s + N_d(1 - \exp - t/T_s)]x\,dx$$

$$+ N_s(x_{c1}(t) - x_{c2}(t))\delta x_d. \tag{26}$$

Solving for $x_{c1}(t) - x_{c2}(t)$

$$\delta w(t) \equiv x_{c1}(t) - x_{c2}(t) = \frac{\delta x_{DD}N_d(x_1 + x_2)(1 - \exp - T_M/2T_S)\exp - t/T_S}{[N_s(x_{c1}(t) + x_{c2}(t) + 2\delta_{xd}) + 2\delta x_d) + N_d(x_{c1}(t) + x_{c2}(t))](1 - \lambda_r \exp - t/T_S)} \tag{27}$$

where

$$\lambda_r \equiv \frac{1}{1 + \dfrac{N_s}{N_d}\left[1 + \dfrac{2\delta x_d}{x_{c1} + x_{c2}}\right]}. \tag{28}$$

Note that λ_r is a parameter that depends on N_d/N_s and V_B.

S_{DDLTS}, the resulting normalized DDLTS signal from the time interval 0 to T_M can be expressed as,

$$S_{DDLTS} \equiv \int_0^{T_M/2} \frac{\delta w(t)\,dt}{T_M} \cdot \frac{2q[N_s\langle w\rangle_r + N_d\langle x_c\rangle_r]}{\delta x_{DD}(T_s = 0)(x_1 + x_2)\cdot N_d}$$

$$= \frac{q[N_s\langle w\rangle_r + N_d\langle w_c\rangle_r]}{\epsilon\delta\lambda_d} \cdot \int_0^{T_M/2} \frac{\delta w(t)\,dt}{T_M}. \tag{29}$$

$\langle w\rangle_r$ and $\langle x_c\rangle_r$ are the average values of w and x_c during the "read" cycle. $\delta x_{DD}(T_s = 0)$ is determined by eqn (22) when $T_s = 0$.

We will assume at this point that the doping concentrations are sufficiently constant and the modulation $\delta_{x\,DD}$ is sufficiently small that λ_d and λ_r are constants. Then after integrating and normalizing this signal we get

$$S_{DDLTS} = \frac{T_S}{T_M}\left[\frac{1 - \exp - T_M/2T_S}{1 - \lambda_d \exp - T_M/2T_S}\right]\frac{1}{\lambda_r}$$

$$\times \ln\left[\frac{1 - \lambda_r \exp - T_M/2T_S}{1 - \lambda_r}\right], \tag{30}$$

For $T_s \gg T_M$, for $\lambda_d \neq 1$ this tends towards

$$S_{\text{DDLTS}} = \frac{1}{2(1 - \lambda_d)(1 - \lambda_r)} \frac{T_M}{T_s}. \quad (31a)$$

When $\lambda_d \to 1$ the corresponding result is

$$S_{\text{DDLTS}} \to \frac{1}{2(1 - \lambda_r)}. \quad (31b)$$

This quantity is plotted in Fig. 8 as a function of T_M/T_S. As long as $N_d \ll N_s$ the spectral responses are similar, but as N_d approaches and exceeds N_s, the sensitivity increases. peaks are shifted to the long time constant spectrum and the curves are broadened. The underlying reason for this effect is the fact that when $N_d \ll N_s$, the deep level feedback term is small and constitutes a small perturbation in the system, but when N_d becomes comparable to N_s, then through feedback it not only modifies its own transient but also affects transients from other deep level species. Because of this essential nonlinearity of the system the effect of λ_r is akin to harmonic distortion of sinusoidal signals: to first order an added component a factor λ_r smaller in strength appears at a time constant $2T_S$. λ_d affects the spectral sensitivity but not the shape of the transient.

We can avoid some of this distortion of the recovery transient if we use a feedback system that balances the capacitance to a constant value during the recovery. This means that x_{c1} and x_{c2} will remain fixed at x_{c0}[14]. Thus no generation of deep level charge will occur for $x > x_{c0}$. This type of measurement will yield a response spectrum of shape characterized by the limit as $\lambda_r \to 0$, but the dependence of δx_{DD} on λ_d will remain. The corresponding normalized signal $S_{cc\text{-DDLTS}}$ for the constant capacitance mode is

$$S_{cc\text{-DDLTS}} \equiv \int_0^{T_M/2} \frac{\delta V_r(t)\, dt}{T_M} \cdot \frac{\epsilon}{qN_d \delta x_{DD}(T_s = 0) \cdot \langle x \rangle_d}$$

$$\equiv \int_0^{T_M/2} \frac{\delta V_r(t)\, dt}{T_M \delta V \lambda_d} = S_{\text{DDLTS}}(\lambda_r = 0) \quad (32)$$

where $\delta V_r(t)$ is the differential voltage required to keep the capacitance constant during corresponding portions of the "read" cycle.

Note that the effect of λ_d is potentially more serious than that of λ_r: as $\lambda_d \to 1$ the spectral response approaches the value $1/2(1 - \lambda_r)$ for large T_S. The effect of $\lambda_d \to 1$ will decrease by one the order of the filter used. In order to avoid having the deep level species in effect "choose" its own value of δx_{DD}, one might use the constant capacitance system to determine the depletion layer edges when both V_1 and V_2 are applied as well as during the recovery transient. This would reduce the effective values of both λ_d and λ_r to zero and would yield the types of spectra we have considered earlier. Another way of suppressing the effects of λ_d would be to make a series of measurements with pulse V_1 and no second pulse. Then make a completely independent set of measurements with a pulse V_2. The differential analysis could be performed later. This procedure is equivalent to making two DLTS measurements and would degrade the effective figure of merit by a factor of $\sqrt{2}$. As is apparent from Fig. 7(c), however, DLTS is also affected by deep level transient distortion during the read cycle. For a self-restored weighting function with no blanking such as one would obtain with a square wave phase sensitive detector; the normalized spectral response is

$$S_{\text{DLTS}} = \frac{T_S}{T_M} \frac{1}{\lambda_r} \ln\left[\frac{(1 - \lambda_r \exp - T_M/2_S)^2}{(1 - \lambda_r)(1 - \lambda_r \exp - T_M/T_S)} \right]. \quad (33)$$

Representative curves are shown in Fig. 8 for comparison with the DDLTS spectral response. For DDLTS if the constant capacitance mode of measurement is not used one expects that $\lambda_d \sim \lambda_r$. Note that for $\lambda_d = \lambda_r = 0.5$ and 0.9 the spectral responses are not identical to those for DLTS, but the basic features are very similar. In the DLTS mode one can suppress all the nonlinearity by using a constant capacitance only during the read cycle, and by performing measurements with different values of V_1 starting from the smallest V_1.
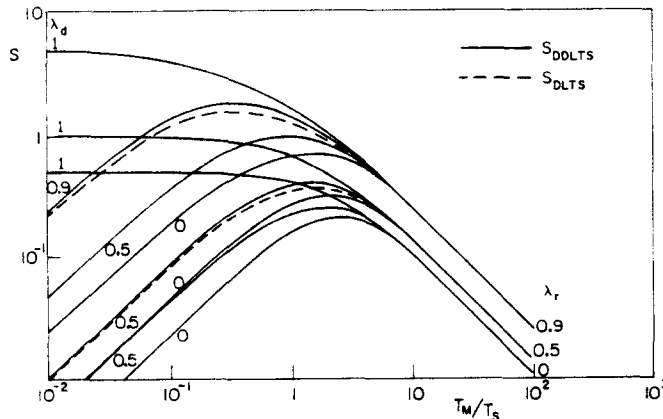

Fig. 8. The distortion of the DDLTS spectrum due to deep level feedback during the capacitive "read" cycle characterized by λ_r and during the drive cycle characterized by λ_d. ————DDLTS. Corresponding DLTS spectra exhibit only "read" distortion———DLTS.

REFERENCES

1. R. Williams, *J. Appl. Phys.* **37**, 3411 (1966).
2. C. T. Sah, L. Forbes, L. L. Rosier and A. F. Tasch Jr., *Solid-St. Electron.* **13**, 759 (1970).
3. D. V. Lang, *J. Appl. Phys.* **45**, 3014, 3023 (1974).
4. H. Lefevre and M. Schulz, *Appl. Phys.* **12**, 45 (1977).
5. T. Coor, *Indust. Res.* **14**, 52 (1972).
6. L. C. Kimerling, *IEEE Trans. Nucl. Sci.* NS-23, 1497 (1976).
7. G. L. Miller, J. V. Ramirez and D. A. H. Robinson, *J. Appl. Phys.* **46**, 2638 (1975).
8. V. Radeka, *Rev. Sci. Instrum.* **38**, 1397 (1967).
9. E. A. Gere and G. L. Miller, *IEEE Trans. Nucl. Sci.* NS-14, 89 (1967).
10. G. L. Miller, D. V. Lang and L. C. Kimerling, *Annual Review of Materials Science*, pp. 377–448, Annual Review Inc. (1977).
11. C. R. Crowell and S. Alipanahi, to be published.
12. K. G. Beauchamp and I. Maddock, *Signal Processing*, pp. 400–466. Wiley, New York (1973).
13. Princeton Applied Research, *Signal Averagers*. Princeton Applied Research, NJ (1977).
14. G. Goto, S. Yanagisawa, O. Wada and H. Takanashi, *Appl. Phys. Lett.* **23**, 150 (1973). Also *J. Appl. Phys.* **13**, 1127 (1974).

APPENDIX A

RMS value of integrated Johnson noise

The mean square thermal (Johnson) noise voltage in a resistor is given by

$$\langle n^2 \rangle = 4kTR\Delta f. \qquad \text{(A1)}$$

If this noise accompanies the incoming signal to a filter, we can estimate the integrated noise over a time interval T_m as follows. A single period component of the noise can be written as

$$\delta n(t) = \sqrt{2}K \sin(\omega t + \phi) \qquad \text{(A2)}$$

where K is the rms amplitude and ϕ a randomly distributed phase. The integrated rms value of the noise over a time T_M averaged over phase and frequency is

$$n_{rms} = \langle \delta n^2(t) \rangle^{1/2}$$

$$= \sqrt{2}K \left[\int_0^\infty \int_0^{2\pi} \int_0^{T_M} \sin(\omega t + \phi)\, dt \right)^2 \frac{d\phi}{2\pi}\, d\omega \right]^{1/2}$$

$$= \sqrt{2}K \left[\int_0^\infty \int_0^{2\pi} \left(\frac{2}{\omega} \sin \omega T_M /2 \sin(\omega T_M/2 + \phi) \right)^2 \frac{d\phi}{2\pi}\, d\omega \right]^{1/2}$$

$$= \sqrt{2}K \left[\int_0^\infty \frac{1}{\pi\omega^2} \sin^2(\omega T_M/2)\, d\omega \right]^{1/2}$$

$$= K\sqrt{T_M}.$$

Therefore

$$N = \frac{n_{rms}}{K} = \sqrt{T_M} \qquad \text{(A3)}$$

APPENDIX B

Normalized signal and noise associated with the weighting functions in Fig. 1 for a signal of the form $\exp(-t/T_s)$: $0 < t < T_m$

1. DLTS
Exponential:

$$w(t) = \exp -(t/T_R) - \alpha \qquad \text{(B1)}$$

where

$$\alpha \equiv \frac{1 - \exp - R}{R}; \quad R \equiv T_M/T_R; \quad x \equiv T_M/T_S.$$

Then

$$S = T_C \left[\frac{1 - \exp - (x + R)}{x + R} - \alpha \frac{1 - \exp - x}{x} \right] \qquad \text{(B2)}$$

$$N = [T_C \alpha((1 + \exp - R)/2 - \alpha)]^{1/2}. \qquad \text{(B3)}$$

Linear ramp:

$$w(t) = 1 - 2t/T_M \qquad \text{(B4)}$$

$$S = T_C[x - 2 + (x + 2)\exp - x]/x^2 \qquad \text{(B5)}$$

$$N = \sqrt{(T_C/3)}. \qquad \text{(B6)}$$

Rectangular: $w(t)$ is

$$1 \text{ when } 0 \le t < \lambda T_M; \; 0 < \lambda < 1$$
$$- \beta \text{ when } \lambda T_M \le t \le T_M \qquad \text{(B7)}$$

where

$$\beta \equiv \lambda/(1 - \lambda);$$

$$S = T_C[1 - \exp - \lambda x - \beta(\exp - \lambda x - \exp - x)]/x \qquad \text{(B8)}$$

$$N = \sqrt{(\beta T_C)}. \qquad \text{(B9)}$$

2. DDLTS
Exponential: $w(t)$ is

$$\exp - t/T_R \text{ when } 0 \le t \le T_M/2$$

and

$$-\exp(R/2) \cdot \exp - t/T_R \text{ when } T_M/2 \le t \le T_M \qquad \text{(B10)}$$

$$S = T_C[1 - \exp - (x/2)] \cdot [1 - \exp(-(x + R)/2)]/(x + R) \qquad \text{(B11)}$$

$$N = \sqrt{T_C}[(1 - \exp - (R))/R]^{1/2}. \qquad \text{(B12)}$$

Square Wave: $w(t)$ is

$$+1 \text{ when } 0 \le t \le T_M/2$$

and

$$-1 \text{ when } T_M/2 \le t \le T_M \qquad \text{(B13)}$$

$$S = T_C[1 - \exp - (x/2)]^2/x \qquad \text{(B14)}$$

$$N = \sqrt{T_C}. \qquad \text{(B15)}$$

Sine:

$$w(t) = \sin(2\pi t/T_M) \qquad \text{(B16)}$$

$$S = T_C 2\pi[1 - \exp - x]/(4\pi^2 + x^2) \qquad \text{(B17)}$$

$$N = \sqrt{(T_C/2)}. \qquad \text{(B18)}$$

Cosine:

$$w(t) = \cos(2\pi t/T_M) \qquad \text{(B19)}$$

$$S = T_C x[1 - \exp - x]/(4\pi^2 + x^2) \qquad \text{(B20)}$$

$$N = \sqrt{(T_C/2)} \qquad \text{(B21)}$$

$T_M/4$ Box-car:

$w(t)$ is

$$+1 \text{ when } T_M/4 \le t \le T_M/2$$

and

$$\qquad \text{(B22)}$$

$$-1 \text{ when } 3T_M/4 \le t \le T_M$$

$$S = T_C \exp - (x/4) \cdot [1 - \exp - (x/4)][1 - \exp - (x/2)]/x \qquad \text{(B23)}$$

$$N = \surd(T_C/2).$$ (B24)

$T_M/10$ Box-car:

$w(t)$ is

$$+1 \text{ when } T_M/10 \leq t \leq T_M/2$$

and (B25)

$$-1 \text{ when } 6T_M/10 \leq t \leq T_M$$

$$S = T_C \exp - (x/10) \cdot [1 - \exp - (2x/5)][1 - \exp - (x/2)]/x$$ (B26)

$$N = \surd(4T_C/5).$$ (B27)

Triangular: $w(t)$ is

$$1 - 4t/T_M \text{ when } 0 \leq t \leq T_M/2$$

and

$$4t/T_M - 3 \text{ when } T_M/2 \leq t \leq T_M$$ (B28)

$$S = T_C[x - 4 + (x + 4)\exp - (x/2)][1 - \exp - (x/2)]/x^2$$ (B29)

$$N = \surd(T_C/3).$$ (B30)

Quadrature Square: $w(t)$ is

$$+1 \text{ when } 0 \leq t \leq T_M/4; \ 3T_M/4 \leq t \leq T_M$$

and

$$-1 \text{ when } T_M/4 \leq t \leq 3T_M/4$$

$$S = T_C[1 - \exp - (x/2)][1 - \exp - (x/4)]^2/x$$ (B32)

$$N = \surd T_C.$$ (B33)